Analysis of the Spatial Distribution of Citrus Bacterial Spot in a Florida Citrus Nursery

T. R. GOTTWALD, Research Plant Pathologist, USDA-ARS, 2120 Camden Rd., Orlando, FL 32803; C. MILLER, Meco Engineering, Oviedo, FL 32765; R. H. BRLANSKY, Associate Professor, Plant Pathology, Citrus Research and Education Center, University of Florida, Lake Alfred 33850; D. W. GABRIEL, Assistant Professor, Department of Plant Pathology, University of Florida, Gainesville 32611; and E. L. CIVEROLO, Research Plant Pathologist, USDA-ARS, Beltsville, MD 20705

ABSTRACT

Gottwald, T. R., Miller, C., Brlansky, R. H., Gabriel, D. W., and Civerolo, E. L. 1989. Analysis of the spatial distribution of citrus bacterial spot in a Florida citrus nursery. Plant Disease 73: 297-303.

The spatial distribution of citrus bacterial spot was analyzed in a central Florida citrus nursery. Detached-leaf bioassay was used to confirm the pathogenicity of bacteria recovered from leaf, stem, and fruit infections, and from leaf washings of symptomatic and asymptomatic leaf tissue. The presence of a bacterium of an undetermined pathovar of *Xanthomonas campestris* on plants at least 3 m beyond plants with visible symptoms was demonstrated by immunofluorescence microscopy and DNA-DNA hybridization probe analysis of leaf washings of asymptomatic tissue. A proposed infection focus of disease was based on visual assessment of disease incidence in a row of 11-yr-old trees to the south of the most heavily infected nursery bed. Isopathic contour mapping further predicted the highest disease incidence in the area of the proposed focus. Computer software was developed to examine the direction of disease spread from a point focus by comparing directional disease gradients. Using the predicted focus, predominant spread was predicted to be east by northeast. The prediction was consistent with patterns of windblown rain observed in the nursery during the previous month.

Considerable attention has been given by pathologists and regulatory agencies to recent outbreaks of a new leaf- and twig-spotting disease of citrus nursery stock in Florida caused by an undetermined pathovar of *Xanthomonas campestris*, termed XC-U. Although similar to (and originally thought to be) citrus bacterial canker disease (citrus canker), caused by *X. campestris* pv. *citri* (Hasse) Dye, the new disease appears to be restricted primarily to citrus nurseries and immature trees recently moved from nurseries to grove situations (16,17). This disease that is similar to citrus bacterial canker was first discovered in September 1984 in a nursery in Polk County, FL, and as of November 1987, has occurred in 36 locations in nine counties in Florida. In an effort to eradicate the new disease, over 20 million infected or exposed trees have been destroyed (17).

The undetermined pathovar of *X. campestris* is serologically and genetically distinct from all other *X. c.* pv. *citri* strains (1,2,5,8). The citrus canker bacterium causes corky, erumpent, water-soaked lesions often surrounded by chlorotic halos on foliage, green wood, and fruit, and can cause defoliation, dieback, and losses in crop quality (2,6,9). In contrast, lesions caused by XC-U are flat or somewhat sunken on foliage. The disease has not been observed to cause defoliation or dieback and has only been found to infect fruit on one occasion (17). The disease has been referred to as Florida nursery canker (17), citrus canker E (8), Xanthomonas leaf spot (16), and citrus bacterial spot (E.

Accepted for publication 20 September 1988 (submitted for electronic processing).

L. Civerolo, *unpublished*).

Whereas *X. c.* pv. *citri* has a fairly broad host range of citrus cultivars and citrus relatives (13), the Florida nursery bacterium appears to preferentially attack trifoliate orange (*Poncirus trifoliata* (L.) Raf.), trifoliate orange hybrids, grapefruit (*Citrus paradisi* Macfad.), or hybrids with one or the other as a parent (16,17,19). Trifoliate orange and its hybrids are primarily used as rootstock varieties. One of the most highly susceptible hosts is cultivar Swingle citrumelo (*P. trifoliata* × *C. paradisi*), a hybrid of two highly susceptible species and a common citrus rootstock (17). Large populations of Swingle citrumelo seedlings are grown in Florida citrus nurseries.

Of the 29 locations where citrus bacterial spot has been found, only two nursery outbreaks, the first in September 1984 and the second in August 1985, exhibited extensive field epidemics. The first was eradicated before data could be collected. The latter was examined and data were collected during the few days between disease confirmation and tree destruction. Eradication in this nursery consisted of the destruction of about 3 million trees (16,17). The purpose of this study was to examine and analyze the spatial distribution of citrus bacterial spot during the August 1985 epidemic, the only extensive field outbreak of this disease for which data exist before 1987. An additional goal was to develop an analytical means of predicting the focus of the epidemic by examining the disease gradient at the point in time when the data were collected.

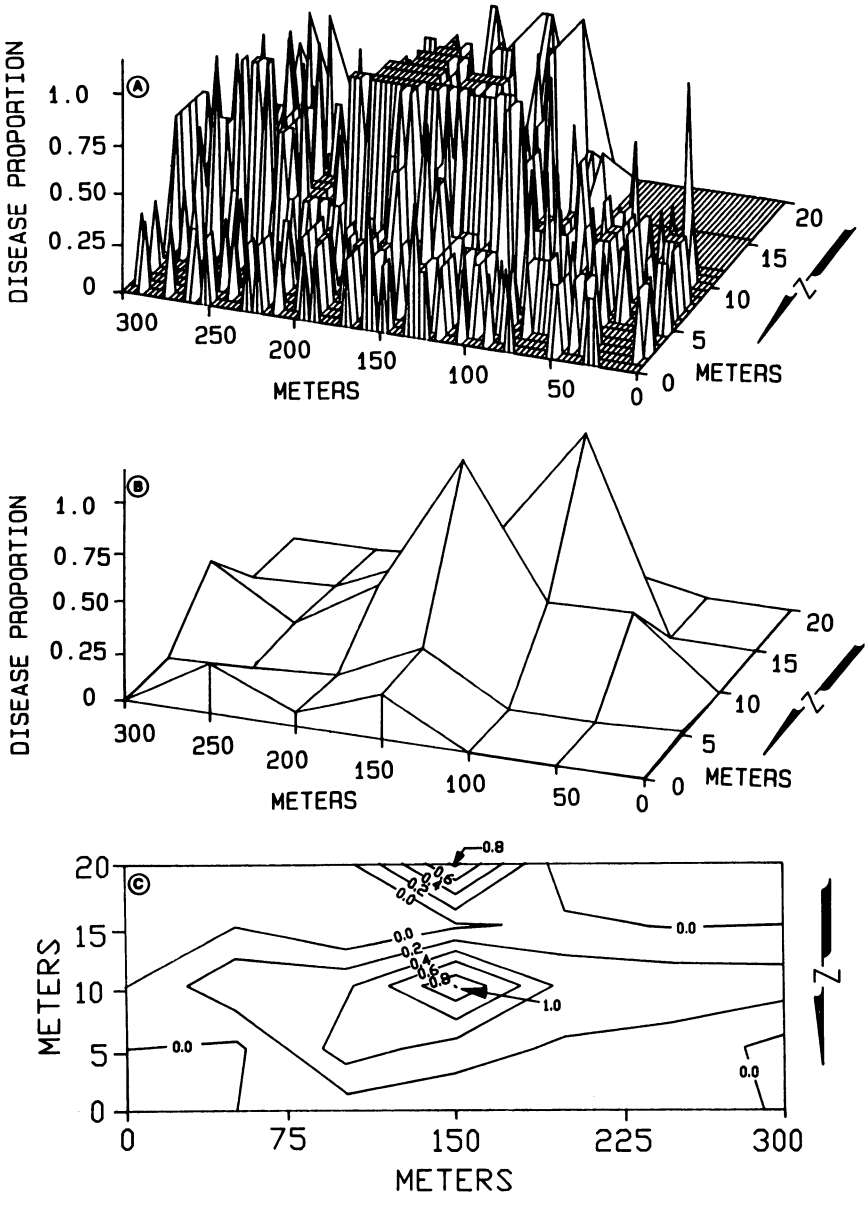

Fig. 1. (A) Three-dimensional response surface of disease incidence of citrus bacterial spot in a central Florida nursery bed (6W) of approximately 32,000 citrus rootstock plants. **(B)** Response surface of the same nursery bed in which individual disease incidence readings are dampened by splining to the three nearest neighbors. **(C)** Isopathic contour map of the splined data predicting relative location of disease fronts at different disease incidence levels.

MATERIALS AND METHODS

Disease manifestation. A 24-ha citrus field nursery with a citrus bacterial spot epidemic (confirmed by the Florida Department of Agriculture and Consumer Services, Division of Plant Industry) was located in Polk County, FL. The nursery consisted of numerous beds of different rootstocks and rootstocks that were bud-grafted with various scions. Trees were arranged in double rows about 300 m long and 0.75 m apart. A single bed, No. 6W, in the southwest corner of the nursery expressed the most severe symptoms of citrus bacterial spot. It was bordered to the south by 11-yr-old trees of *P. trifoliata* 'Flying Dragon' used as rootstock seed source trees, to the north and east by other nursery beds of mixed rootstocks and scions, and to the west and south by adjacent property with mature citrus. The bed consisted of approximately 32,000 rootstock seedlings, about 0.75–1.0 m tall, spaced about 15 cm apart in 16 rows. The first 10 rows nearest the Flying Dragon trees were planted with Swingle citrumelo rootstock and the six rows farthest from the Flying Dragon trees were planted with cultivar Carrizo citrange (*P. trifoliata* × *C. sinensis* (L.) Osbeck). Many of the plants in the row of Swingle nearest the Flying Dragon trees were bud-grafted, the buds were wrapped, and the tops were cut back. Thus, these plants were not included in the analysis.

Due to the large number of plants in the bed, the proportion of disease of 20 contiguous plants in each row was assessed as a group (number of diseased plants per 20). Disregarding groups of missing plants in the first row, 1,883 individual disease incidence readings were obtained. The disease incidence of adjacent Flying Dragon trees was assessed on an individual-tree basis. The average width of the canopy of the Flying Dragon trees within the row was approximately equivalent to the length of 20 Swingle citrumelo seedlings in a nursery row.

Detection of bacteria and disease confirmation. Pathogenicity of bacteria from lesions and presence of epiphytic bacteria from asymptomatic leaf tissue (from the same plant unless otherwise specified) was determined via detached-leaf assay (E. L. Civerolo, *unpublished technique*). Five leaves from each sample plant were combined and washed in 50 ml of sterile distilled water in 250-ml flasks on a rotating shaker for 45 min. The wash solution was assayed on young leaves of Swingle, Duncan grapefruit, and/or Mexican lime (*C. aurantifolia* (Christm.) Swingle) seedlings, one-half to three-fourths expanded. Leaves were surface-disinfested in 1% sodium hypochlorite for 3 min, then rinsed thoroughly twice with sterile distilled water. The leaves

were then laid aseptically on 1% water agar, ventral side up, were wounded by puncturing with a sterile needle five times on each side of the midrib, and 20 μl of the leaf-wash water was pipetted onto each of the 10 wounds. Two strains of XC-U, X169-1 from a previously related citrus bacterial spot outbreak, and X4600, a confirmed XC-U from the nursery under investigation but isolated a few days before this study, were used as controls. Each strain was grown in nutrient broth for 24 hr, centrifuged, and the pellet was resuspended in sterile distilled water. Then 20 μl of the resuspension (about 10^5 cfu) was pipetted onto each of 10 needle wounds of a detached leaf as above. If bacteria were present 7–10 days later, water-soaked lesions developed on inoculated, detached leaves. The number of lesions per leaf was recorded. Additional field samples consisting of symptomatic leaf tissue with lesions and asymptomatic tissue from leaves apparently free of disease were cut from foliage with a 2.5-mm cork borer. Lesions on fruit and stems were excised with a scalpel. Individual leaf disks and excised tissue were soaked in 3 ml of sterile distilled water for approximately 30 min. These samples were assayed via detached-leaf assay as above. Ten detached-leaf assays were conducted per sample.

The remainder of the leaf-wash solutions from above were assayed via DNA-DNA hybridization probe (DNA probe) by drawing the wash solution down onto 47-mm-diameter, cellulose acetate/nitrate filters. The filters were placed onto the agar surface of a semiselective medium (11) and were incubated for 24 hr to preferentially enhance the growth and formation of microcolonies of XC-U on the filter surface while inhibiting background bacteria. Each filter was floated on about 10 ml of 0.5 M NaOH, 1.5 M NaCl for 15 min to lyse all bacteria and denature the bacterial DNA. Filters were neutralized with 3 M NaCl and 0.5 M Tris-HCl (pH 7.1–7.5) for 15 min, soaked on 0.3 M NaCl containing 0.03 M sodium citrate in water, and baked for 2 hr at 55 C. Denatured and neutralized samples on filters were hybridized for at least 6 hr with ^{32}P-labeled DNA probe XCT11-85, washed, and autoradiographed as described previously (5). Results were recorded as the number of microcolonies (positive signals) per filter. There is some cross-reaction of the DNA probe with a few other xanthomonads. Therefore, the test is inconclusive in itself and was used here as a presumptive test for suspect epiphytic bacteria only.

Other leaf disks taken from the same plants were assayed via membrane entrapment and immunofluorescence microscopy (IFM) (1). For IFM tests, two 5-mm leaf disks from each sample leaf were pooled by sample and fixed in 3% glutaraldehyde in 0.066 M phosphate buffer (pH 6.8) for about 48 hr. The leaf disks were then rinsed three times in phosphate-buffered saline containing 0.2% sodium azide. Disks were chopped in one or two drops of distilled water with a single-edged razor blade, diluted with 2 ml of distilled water, and mixed vigorously for approximately 15 sec. The preparation was centrifuged at low speed for 5 min to pellet the plant debris. The supernatant was forced through a Nucleopore 25-mm Swin-Lok double filtration apparatus (Nucleopore Corp., Pleasanton, CA) containing a 5.0-μm polycarbonate prefilter to remove large-cell debris, followed by a 0.2-μm black polycarbonate membrane filter to trap the bacteria. The polycarbonate filter was incubated with fluorescent-labeled IgG to XC-U for 1–2 min. The membrane was washed in buffer to remove excess stain and then mounted on a glass microscope slide and viewed at 1,000× under oil with epifluorescence (546–590 nm) for the presence of XC-U bacteria. The IFM assay was tested against eight other pathovars of *X. campestris*, including 12 strains and five *X. c.* pv. *citri* strains (Brlansky, *unpublished data*). All produced negative or weak (heterologous) reactions, whereas tests against four XC-U isolates all produced strong (homologous) reactions. This is indicative of a high degree of specificity of the polyclonal antisera used in the assay (1). Therefore, results were interpreted as +/− for the presence or absence of XC-U bacteria based on a comparison of homologous versus heterologous or no reaction to the labeled polyclonal IgG on + and − control slides.

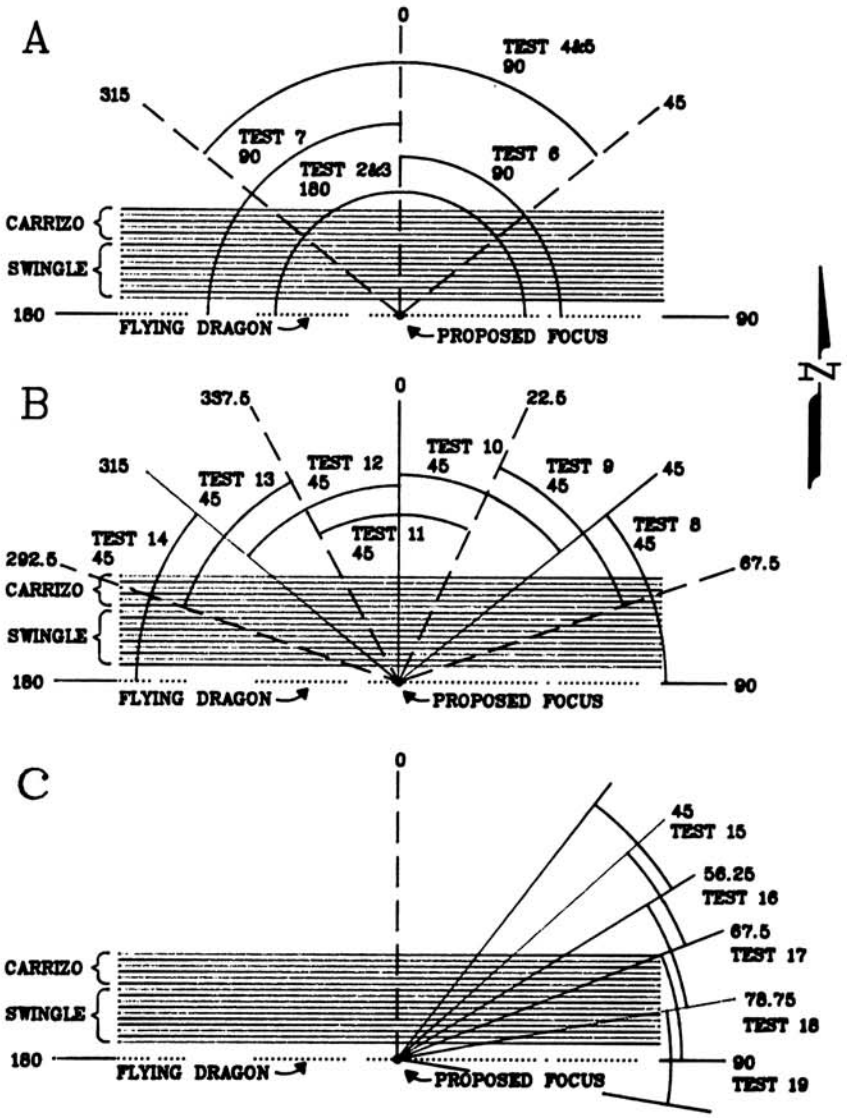

Fig. 2. Graphic representation of disease gradient analysis by direction, as reported in Table 3, showing orientation of nursery bed infested with citrus bacterial spot and position of proposed focus of disease. **(A)** Directional analysis of disease gradients (tests 2–7). Arcs represent the angle of the sector tested (tests 2 and 3 represent the gradient analysis of the whole plot arc = 180°, tests 4–7 represent the gradient analysis of subsets of the plot described by arcs of 90° in different magnetic headings). **(B)** Directional analysis of plot (tests 8–14) in which different directions are tested within arcs of 45°. **(C)** Directional analysis of plot (tests 15–19) in which different directions are tested within arcs of 22.5°.

Analysis of spatial data. Aggregation or randomness of disease was determined by ordinary runs analysis (10). Analysis was performed in two directions by examining the data within rows (east-west) and across rows (north-south). A nonrandom aggregation or "clustering" of diseased trees was assumed if the observed number of runs was less ($P = 0.05$) than the expected number of runs for a given disease value.

Three-dimensional representation of the relative position and disease incidence of groups of plants was prepared with the aid of SAS graphics G3D procedure (15) (Fig. 1A). In an attempt to visualize locations of concentrations of disease within the plot, and thus potential foci of disease, the "near" option of SAS G3GRID procedure was used to estimate a bivariate fifth-degree polynomial to the three nearest neighbors (15) (Fig. 1B). The output data set from this procedure were further analyzed via the SAS GCONTOUR procedure to estimate the "isopathic lines" of disease incidence (those lines describing the relative position of the advancing disease at different incidence levels) (15) (Fig. 1C).

Computer program development. In order to test directional spread from a focal point of disease by comparing disease gradients, a program was developed by Meco Engineering of Oviedo, FL (in conjunction with the first author), to calculate average disease incidence of trees at definable increments of distance from a projected point focus. The program enabled definition of 1) the direction of spread and 2) the angle of a wedge whose apex was the focus and that was bisected by the vector, indicating the direction of spread tested. All points within this wedge (subset) were considered in the analysis. The distance increment was also user-definable and described sectors or bands of different radii from the focus whose ends were defined by the angular limits of the wedge (Fig. 2). The disease proportion of plants within these defined "sectors" was averaged, and output was an average disease proportion per distance increment. The program was used to investigate gradients of disease from a proposed focus of infection within wedges of different angles and in different directions.

The disease proportion data from the above program were weighted inversely by dividing the average disease proportion of each sector by the number of plants within that sector. This weighting was necessary to adjust for the increasing number of observations within sectors farther from the test focus. A series of linearizing models was tested on both unweighted and weighted data. The models tested were: 1) linear (Y) vs. linear (X), 2) $\log_{10}$ (Y) vs. $\log_{10}$ (X), 3) probit (Y) vs. probit (X), 4) $\log_{10}$ (Y) vs. linear (X), 5) linear (Y) vs. logit (X), 6) linear (Y) vs. probit (X), and 7) probit (Y) vs. linear (X), where X = distance from the focus in meters and Y = the disease incidence expressed as 0–1.0. All models were evaluated by linear regression.

RESULTS AND DISCUSSION

Based on visual inspection of the entire nursery, the highest concentration of disease was located in the southwest corner of the nursery and, in particular, in nursery bed 6W. Citrus bacterial spot lesions also occurred on foliage, stems, and fruit of 11-yr-old Flying Dragon seed trees along the southern edge of bed 6W (Fig. 3A–C). Citrus bacterial spot lesions on the Flying Dragon plant parts were examined closely and many stem lesions on wood were estimated to be 6–12 mo old, or possibly older (Fig. 3B). Lesions on infected Swingle foliage and stems in adjacent bed 6W were restricted to growth no more than 2–3 mo old (Fig. 3D). Thus, the Flying Dragon trees were probably acting as the source of the nursery bed citrus bacterial spot epidemic. There was no evidence of disease in any older wood; only immature green wood is susceptible to this disease. No conclusions were possible as to the origin of the inoculum that caused the disease on the Flying Dragon trees.

Bacteria of XC-U were detected on the phylloplane of both symptomatic and asymptomatic plant parts from all samples assayed via IFM and DNA probe (Table 1). Recovery of pathogenic bacteria from all symptomatic Swingle leaf tissue in nursery bed 6W was confirmed via detached-leaf assay. In one case, asymptomatic leaf tissue from bed 6W resulted in positive detection of epiphytic XC-U bacteria by IFM and DNA probes. However, this could not be confirmed via detached-leaf assay. An occurrence of a single XC-U lesion on a Swingle plant in bed 8W, two beds north of bed 6W (about 40 m), was confirmed via IFM and DNA probes, as was the presence of XC-U on the phylloplane of asymptomatic leaf tissue from the same plant and plants 1–3 m away (Table 1). The ability of IFM and the DNA probes to detect low concentrations of phylloplane bacteria may be indicative of their usefulness to detect the pathogen in absence of disease symptoms or in subclinical infections. Therefore, these detection techniques are useful as potential screening assays to confirm pathogen-free nursery stock.

Disease on 53 of the 129 Flying Dragon trees ranged from one to numerous lesions per tree. A single tree just east of the center of the row of trees was estimated to be both the most severely infected and to have the oldest lesions on wood.

Three-dimensional representation of disease incidence splined to the nearest three neighbors in nursery bed 6W and the adjacent row of Flying Dragon trees revealed two major peaks (Fig. 1B). These peaks corresponded to 1) the location of the most severely infected Flying Dragon tree and its nearest neighbors and 2) an area in the center of nursery bed 6W. The analysis is based on the assumption that areas with the highest average disease incidence have been infected longer than those with

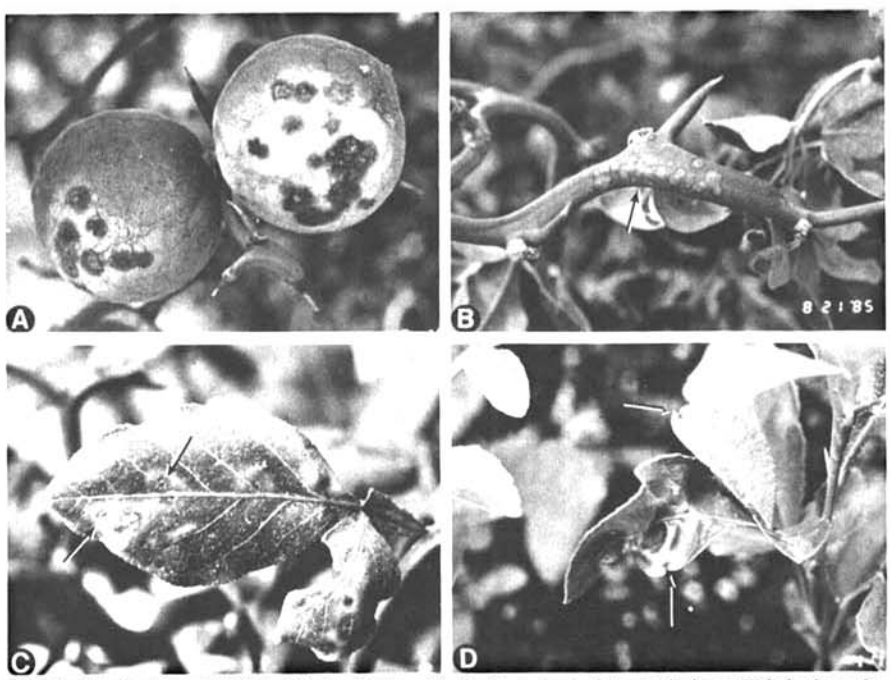

Fig. 3. (A) *Poncirus trifoliata* 'Flying Dragon' fruit citrus bacterial spot lesions. This is the only known case in which fruit of any citrus or citrus relative has become infected with an undetermined pathovar of *Xanthomonas campestris*. **(B)** Twig of Flying Dragon expressing symptoms of citrus bacterial spot. Note water-soaked margins of individual lesions. **(C)** Mature Flying Dragon leaf with old citrus bacterial spot lesions. **(D)** Cultivar Swingle citrumelo leaf with marginal citrus bacterial spot lesions. Note leaf distortion associated with infection.

lower disease incidence. Although this is usually true, disease incidence can also be affected by cultivar susceptibility and environmental factors.

The isopathic contour map further identified these two areas as potential epicenters of disease (Fig. 1C). The age of the infected tissue in the most severely infected Flying Dragon tree compared with the age of the infected tissue in the center of the Swingle nursery bed points to the Flying Dragon tree as the most likely primary focus of infection in the nursery. Lack of detectable disease on older wood may have been indicative of a recent introduction of citrus bacterial spot into the Flying Dragon trees and, thus, into the nursery. The possibility exists that the disease could have been introduced in a previous set of nursery trees that acted as a source of inoculum to infect the Flying Dragon trees before the time those nursery trees were sold and removed from the nursery.

Ordinary runs analysis of bed 6W indicated a nonrandom distribution of diseased plants in 18 of 20 rows (east-west) analyzed. For the row of Flying Dragon trees analyzed, the analysis indicated a nonrandom aggregation in that row as well. When bed 6W was examined across rows (north-south), a nonrandom distribution of diseased plants was indicated in 11 of the 16 tests (Table 2). The slightly greater aggregation of diseased plants within rows than across rows may be indicative of a higher rate of spread within rows due to the closer spacing of susceptible individuals.

The probit transformation was found to be quite useful in linearizing the derived dispersal gradient data. Linear regression of probit (Y) vs. probit (X) resulted in the highest coefficients of determination for those models tested in 11 out of 19 cases, and probit (Y) vs. linear (X) in four out of 19 cases (Table 3). However, the probit (Y) vs. linear (X) accounted for only 0.002–0.007% more of the variation associated with regression in the four cases where it was superior to the probit (Y) vs. probit (X) model. The probit (Y) vs. probit (X) model was thus used for comparison of all data from the analysis of directional spread and accounted for 0.891–0.998% of the variation associated with regression in 18 of the 19 cases tested (Table 3). One benefit of the probit (Y) vs. probit (X) model is the ability to include disease incidence values of 0% without adjusting the data, because it does not include a logarithm function in the transformation. The log-log model cannot be used with disease incidence readings of 0 (7), and modifications have been suggested to improve the original model (12). An additional benefit of the probit (Y) vs. probit (X) model is the increased accuracy of the disease gradient slope by accentuating differences between slopes that are more nearly similar when other models such as log (Y) vs. log (X) are employed.

A common method to calculate a disease gradient across a plot from a line or block source of inoculum is to calculate an average disease incidence for each row of plants within the block and regress this against the distance of the corresponding rows for the source (3,4). Test 1 corresponds to such an analysis (Fig. 2, Table 3). The disease proportion, taking the plot as a whole, was 0.450. This was the only case of the 19 tested in which the probit (Y) vs. probit (X) model was less appropriate. The best model in this case was the linear (Y) vs. linear (X) model. The slope predicted by the probit (Y) vs. probit (X) model was shallow (−0.0004), and the r^2 value of 0.588 was low in comparison with the linear (Y) vs. linear (X) model. The inability of those models tested to describe the disease gradient in this case was related to the average disease incidence calculated from entire rows of trees. Average disease incidence by row resulted in sharply decreasing disease incidence relative to the hypothesized source of infection of rows at, and immediately adjacent to, the focal row and again at the farthest

Table 1. Immunofluorescence, DNA-DNA hybridization probe, and detached-leaf assay of samples taken from a central Florida nursery infected with citrus bacterial spot

Sample source[a]	IFM[b]	DNA probe[c]	Percent infection by detached-leaf assay[d]		
			Duncan grapefruit	Mexican lime	Swingle citrumelo
Swingle (bed 6W), row 6, north of center of plot					
Symptomatic	+	0	100	100	100
Asymptomatic	+	3	100	0	3
Swingle (bed 6W), center of plot					
Symptomatic	+	3	100	0	100
Asymptomatic	+	9	N	N	N
Symptomatic	+	10	100	10	0
Asymptomatic	+	2	0	0	0
Swingle (bed 8W), near road					
Asymptomatic	+	1	N	N	N
Symptomatic (same plant)	+	7	0	0	0
Plant 1 m from last infection	+	0	0	0	0
Plant 2 m from last infection	+	3	0	0	0
Plant 3 m from last infection	+	1	0	0	0
Flying Dragon					
Leaf sample, "hot spot"	+	9	100	75	100
Stem isolations	N	TNTC	100	100	N
Leaf isolations	N	TNTC	N	100	N
Fruit isolations	N	TNTC	N	100	N
Swingle (bed 6W), isolations soaked for 1 hr					
One lesion	N	N	100	N	100
Two lesions	N	N	100	N	100
Three lesions	N	N	100	N	100
Four lesions	N	N	50	N	100
Five lesions	N	N	50	90	100
Culture controls of undetermined pathovar of *Xanthomonas campestris*					
X169-1 (previous outbreak)	N	N	60	30	67
X4600 (same outbreak)	N	N	100	N	100
Immunofluorescence controls					
Positive	+				
Negative	−				

[a] Samples from cultivar Swingle, bed 6W, were taken from about 10 m north of the center of the plot and from near the center of the plot. Each sample consisted of five leaves either with or without symptoms taken from five different plants. Samples from Swingle, bed 8W, were taken at the visual limit of symptom expression. Samples consisted of four symptomatic and four asymptomatic leaves from the last plant with visual symptoms farthest north from bed 6W and four asymptomatic leaves from plants 1–3 m to the north of this plant. Samples from cultivar Flying Dragon consisted of random diseased leaves, stems, and fruits near the center of the row from which isolations were made from excised lesions soaked for about 5 min in sterile distilled water. Samples from isolations of Swingle, bed 6W, consisted of diseased leaves collected randomly from near the center of the plot, whose lesions were excised and soaked in vials of distilled water containing one, two, three, four, or five lesions each for 1 hr.

[b] Immunofluorescence microscopy, where + = positive detection of fluorescent-labeled XC-U (one or more labeled bacteria found), − = no labeled bacteria found, and N = not tested.

[c] Number of suspect microcolonies of the undetermined pathovar of *Xanthomonas campestris* per microfilter by detected DNA-DNA hybridization probe; TNTC = too numerous to count, N = not tested.

[d] Percentage of inoculations that resulted in disease reactions by detached-leaf assay; 0 = no reaction by any inoculation, N = not tested. Readings on each cultivar represent an average for three replicates of 10 inoculations per replicate.

distances from the focus, and relatively level or slightly higher disease incidence of rows midway in the distribution. This roughly descending stair-steplike distribution of disease incidence was poorly linearized by all models tested that tend to best linearize sigmoid curves (20). Therefore, the probit (Y) vs. probit (X) model would be the best to linearize disease gradients of an expanding wave front of disease, such as the bacterial epidemic described here, which assumes a roughly descending stair-steplike gradient before transformation.

Directional disease gradients were investigated in a series of tests using the Flying Dragon tree with the highest incidence of disease as the disease focus (Table 3). This tree was also indicated as the potential epicenter of the outbreak by isopathic contour mapping. The software described above provided a means to examine disease gradients in various directions from the potential focus, and to narrow the angle of the wedge (subset) in an attempt to identify the dominant direction of disease spread. Tests 2 and 3 examined the gradient of the entire plot emanating from the proposed focus at the south side of the plot (Fig. 2, Table 3). Although not much difference was seen in decreasing the resolution of the test from 5 to 10 m, both analyses resulted in superior fits of the gradient curves to that of test 1, which used the disease incidence of entire rows and the Flying Dragon row as a line source. Tests 4–7 examine the data in three directions with arcs reduced to an angle of 90°. The flattest slope of all models tested, indicative of the predominant direction of spread and the best r^2, was in the northeast direction (test 6), 45° east of magnetic north. Tests 8–14 examine the data in seven directions with a further reduction in the angle of the arc to 45° (Fig. 2, Table 3). The flattest slope, and thus a better prediction of the predominant angle of disease spread by all but two models tested, was from test 8 in the east-by-northeast direction, 67.5°. A final analysis was performed examining disease gradients in the east-by-northeast direction with a series of five separate analyses (tests 15–19), each describing arcs of 22.5° and separated by 11.25° (Fig. 2C). The flattest slope predicted by five of the eight models tested was 56.25° east of north, followed by 67.5°, predicted by three out of eight models. Thus, the best prediction indicated that disease spread was predominantly to the east-by-northeast direction.

Rain showers with moderate-to-high winds are common in central Florida during spring and summer. Personnel associated with the diseased nursery indicated that such blowing rainstorms passed through the nursery on more than one occasion during the 2–3 mo directly preceding the citrus bacterial spot outbreak. The spread of *X. c.* pv. *citri* is thought to be directly associated with the blowing rainstorms (9,14,18,19). Therefore, it is likely that XC-U bacteria manifesting a similar disease could be disseminated in a similar manner. Although the predominant airflow across central Florida in spring and summer is east and northeast, local wind patterns are at times influenced by numerous factors, and blowing rainstorms are occasionally recorded as originating from many directions. During the 2–3 mo before the discovery of the citrus bacterial spot epidemic, storms passed over the nursery in the predominantly north and east directions. Thus, the pattern of disease in the field, recorded during the examination of this disease outbreak, could be explained by the occurrence of one or more such blowing rain events.

Added in galley: Since acceptance, the authors recognize the publication of a new taxonomic designation for the causal organism of citrus bacterial spot: *Xanthomonas campestris* pv. *citrumelo* (Gabriel) pv. nov. (Gabriel, D. W., Kingsley, M. T., Hunter, J. E., and Gottwald, T. R. 1989. Reinstatement of *Xanthomonas citri* (ex Hasse) and *X. phaseoli* (ex Smith) to species and reclassification of all *X. campestris* pv. *citri* strains. J. Syst. Bacteriol. 39:14-22.)

Table 2. Ordinary runs analysis of a citrus bacterial spot infected nursery bed

Disease incidence (%)	Observed	Expected	Standard deviation	Z[a]	P[b]	Aggregation of diseased plants
		Rows (east-west)[c]				
34	28	35.8	3.962	−1.846	0.0326	+
34	23	35.2	3.892	−3.009	0.0013	+
45	19	38.6	4.281	−4.457	0.0000	+
56	20	38.0	4.238	−4.120	0.0000	+
47	21	39.3	4.340	−4.110	0.0000	+
47	25	40.3	4.398	−3.375	0.0004	+
45	17	38.6	4.281	−4.924	0.0000	+
53	30	39.3	4.330	−2.036	0.0209	+
74	14	30.5	3.345	−4.775	0.0000	+
78	10	27.4	2.990	−5.651	0.0000	+
72	15	32.6	3.543	−4.824	0.0000	+
84	13	21.3	2.266	−3.425	0.0003	+
65	20	36.3	3.966	−3.986	0.0000	+
51	27	38.5	4.300	−2.557	0.0052	+
35	29	36.31	3.966	−1.716	0.0431	+
22	23	27.5	2.981	−1.340	0.0901	−
36	27	36.9	4.033	−2.330	0.0099	+
23	27	28.6	3.106	−0.349	0.3635	−
13	10	16.7	1.827	−3.85	0.0000	+
21	13	49.9	2.474	−2.569	0.0051	+
		Subplots (north-south)[c]				
16	23	27.8	2.659	−1.628	0.0518	−
19	33	31.7	3.051	+0.587	0.0786	−
22	33	35.2	3.406	−0.506	0.2877	−
31	36	43.6	4.250	−1.667	0.0478	+
33	34	45.0	4.394	−2.390	0.0084	+
15	23	26.5	2.520	−1.172	0.1206	−
27	25	40.3	3.916	−3.772	0.0001	+
68	30	43.6	4.25	−3.078	0.0010	+
76	19	36.3	3.516	−4.781	0.0000	+
78	28	34.1	3.29	−1.698	0.0448	+
80	22	31.7	3.051	−3.018	0.0013	+
67	29	44.3	4.324	−3.425	0.0003	+
63	32	46.3	4.57	−3.015	0.0013	+
51	38	43.49	4.582	−1.090	0.1379	−
56	28	35.5	4.098	−1.719	0.0428	+
49	15	26.5	3.53	−3.110	0.0009	+
		Focus[d]				
70	16	30.6	3.47	−4.050	0.0000	+

[a] Standardized variable; large negative numbers indicate a nonrandom distribution of diseased plants.
[b] Significance level; levels of $P \leq 0.05$ were considered indicative of a nonrandom distribution of diseased plants.
[c] Plot was subdivided into 20 rows (east-west) and 16 subplots (north-south) across rows.
[d] Focus = row of 11-yr-old cultivar Flying Dragon trees.

ACKNOWLEDGMENTS

We wish to extend our appreciation to the Florida Department of Agriculture and Consumer Services, Division of Plant Industry, and USDA-APHIS, for their cooperation in allowing us to investigate this outbreak before its eradication, and for subsequent information about it. We thank C. L. Schoulties and R. E. Stall for their aid in field identification and consultation, and A. Dow and S. Cullen for their untiring efforts in field data collection and sample analysis.

LITERATURE CITED

1. Brlansky, R. H., Lee, R. F., and Civerolo, E. L. 1986. Detection of *Xanthomonas campestris* from citrus by membrane entrapment and immunofluorescence. (Abstr.) Phytopathology

Table 3. Directional disease gradient analysis[a] of citrus bacterial spot in an infested citrus nursery in central Florida

Proposed direction of spread tested in degrees[b]	Angle of arc tested[c]	Resolution (m)[d]	No. of counts in test arc	No. of disease counts in test arc	Disease proportion	Model tested: Linear (*Y*) vs. linear (*X*)		Log (*Y*) vs. log (*X*)		Probit (*Y*) vs. probit (*X*)		Log (*Y*) vs. linear (*X*)		Linear (*Y*) vs. logit (*X*)		Linear (*Y*) vs. probit (*X*)		Probit (*Y*) vs. linear (*X*)	
						r^2	Slope	r^2	Slope	r^2	Slope	r^2	Slope	r^2	Slope	r^2	Slope	r^2	Slope
0	NA	NA	NA	NA	0.450	.588	−.0004	.135	−.143	.006	−.0005	.145	−.0008	.649	−.073	.533	−.0004	.006	+.0005
0	180	5	1,584	713	0.450	.262	−.0001	.745	−.774	.970	−.105	.635	−.023	.593	−.007	.253	−.0001	.965	−.098
0	180	10	1,584	713	0.450	.343	−.0001	.881	−.781	.965	−.082	.678	−.010	.727	−.006	.340	−.00007	.965	−.080
0	90	2	98	63	0.643	.528	−.047	.892	−1.882	.992	−527.59	.828	−.893	.677	−.257	.414	−43.488	.995	−.503
0	90	3	98	63	0.643	.499	−.049	.938	−1.942	.989	−530.60	.789	−.908	.650	−.274	.429	−47.573	.996	−.512
45	90	10	833	419	0.503	.314	−.0001	.762	−.579	.962	−.107	.657	−.013	.519	−.004	.311	−.0001	.961	−.104
315	90	10	866	360	0.416	.510	−.0001	.757	−.981	.891	−.108	.780	−.015	.780	−.009	.503	−.0001	.887	−.105
67.5	45	10	776	378	0.872	.278	−.0002	.816	−.864	.979	−.327	.642	−.037	.506	−.006	.272	−.0002	.981	−.301
45	45	3	98	59	0.602	.346	−.015	.719	−1.266	.984	−514.22	.745	−.609	.376	−.078	.221	−12.916	.982	−.492
22.5	45	2	57	41	0.719	.595	−.048	.846	−1.629	.992	−527.57	.869	−.890	.689	−.244	.474	−43.491	.981	−.486
0	45	2	40	30	0.750	.700	−.053	.755	−.273	.998	−257.08	.891	−.867	.660	−.226	.427	−43.686	.798	−.219
337.5	45	2	57	36	0.632	.590	−.048	.828	−1.655	.992	−527.58	.869	−.894	.670	−.247	.414	−43.491	.980	−.488
315	45	5	98	69	0.704	.449	−.005	.637	−.848	.979	−.489	.782	−.189	.356	−.025	.443	−.007	.967	−.356
292.5	45	10	759	308	0.406	.289	−.0004	.907	−.326	.972	−.548	.642	−.059	.757	−.011	.277	−.0004	.975	−.482
45	22.5	10	651	269	0.413	.404	−.0006	.909	−1.349	.789	−.685	.742	−.088	.711	−.011	.397	−.0007	.779	−.593
56.25	22.5	10	708	336	0.475	.355	−.0003	.877	−1.075	.991	−.463	.742	−.055	.606	−.008	.343	−.0004	.988	−.416
67.5	22.5	10	176	89	0.506	.310	−.002	.419	−.009	.919	−1.403	.627	−.173	.221	−.012	.318	−.003	.902	−1.019
78.75	22.5	3	70	42	0.600	.472	−.019	.650	−1.279	.996	−514.95	.882	−.694	.488	−.093	.305	−16.30	.960	−.474
90	22.5	3	42	28	0.667	.636	−.035	.821	−1.288	.987	−522.1	.881	−.769	.624	−.159	.334	−27.761	.926	−.460

[a] In tests 2–7, arcs represent the angle of the sector tested (tests 2 and 3 represent the gradient analysis of the whole plot arc = 180° and tests 4–7 represent the gradient analysis of subsets of the plot described by arcs of 90° in different magnetic headings). Different directions are tested within arcs of 45° for tests 8–14 and 22.5° for tests 15–19.
[b] Direction of spread tested is given in degrees of the compass relative to magnetic north (0°).
[c] Arc tested consists of two lines radiating at a given angle from a proposed focal point (if the proposed direction of spread is 315° from magnetic north [NW], and the arc tested is 45°, all plants between lines radiating at 292.5° and 337.5° from the proposed focal plant are included in the analysis, including those points that fall on these lines).
[d] Resolution is the width in meters of concentric bands of trees radiating from the proposed focal tree (a resolution of 3 m describes concentric bands 3 m wide radiating from a central focal tree). The disease proportion of all plants that fall within the band and between the lines of the prescribed arc is averaged to establish an average disease proportion at that distance from the focal tree.

76:1101.
2. Civerolo, E. L. 1984. Bacterial canker disease of citrus. J. Rio Grande Val. Hortic. Soc. 37:127-146.
3. Danós, E., Berger, R. D., and Stall, R. E. 1984. Temporal and spatial spread of citrus canker within groves. Phytopathology 74:904-908.
4. Danós, E., Bonazzola, R., Berger, R. D., Stall, R. E., and Miller, J. W. 1981. Progress of citrus canker on some species and combinations in Argentina. Proc. Fla. State Hortic. Soc. 94:15-18.
5. Gabriel, D. W., Hunter, J. E., Kingsley, M. T., Miller, J. W., and Lazo, G. R. 1988. Clonal population structure of *Xanthomonas campestris* and genetic diversity among citrus canker strains. Mol. Plant Microbe Interact. 1:59-65.
6. Gottwald, T. R., McGuire, R. G., and Garran, S. 1988. Asiatic citrus canker: Spatial and temporal spread in simulated new planting situations in Argentina. Phytopathology 78:739-745.
7. Gregory, P. H. 1968. Interpreting plant disease dispersal gradients. Annu. Rev. Phytopathol. 6:189-212.
8. Hartung, J. S., and Civerolo, E. L. 1987. Genomic fingerprints of *Xanthomonas campestris* pv. *citri* strains from Asia, South America, and Florida. Phytopathology 77:282-285.
9. Koizumi, M. 1985. Citrus canker: The world situation. Pages 2-7 in: Citrus Canker: An International Perspective. L. W. Timmer, ed. Proc. Symp. Inst. Food Agric. Sci., University of Florida.
10. Madden, L. V., Louie, R., Abt, J. J., and Knoke, J. K. 1982. Evaluation of tests for randomness of infected plants. Phytopathology 72:195-198.
11. McGuire, R. G., Jones, J. B., and Sasser, M. 1986. Tween media for semiselective isolation of *Xanthomonas campestris* pv. *vesicatoria* from soil and plant material. Plant Dis. 70:887-891.
12. Mundt, C. C., and Leonard, K. J. 1985. A modification of Gregory's model for describing plant disease gradients. Phytopathology 75:930-935.
13. Peltier, G., and Frederich, W. J. 1924. Further studies on the relative susceptibility to citrus canker of different species and hybrids of the genus *Citrus*, including the wild relatives. J. Agric. Res. 28:227-239.
14. Reedy, B. C. 1984. Incidence of bacterial canker of citrus in relation to weather. Geobios New Rep. 3:39-41.
15. SAS Institute, Inc. 1985. SAS/GRAPH Users Guide Version 5. SAS Institute, Inc., Cary, NC. 596 pp.
16. Schoulties, C. L., Civerolo, E. L., Miller, J. W., Stall, R. E., Krass, C. J., Poe, S. R., and DuCharme, E. P. 1987. Citrus canker in Florida. Plant Dis. 71:388-395.
17. Schoulties, C. L., Miller, J. W., Stall, R. E., Civerolo, E. L., and Sasser, M. 1985. A new outbreak of citrus canker in Florida. Plant Dis. 69:361.
18. Serizawa, S., and Inoue, K. 1975. Studies on citrus canker III. The influence of wind blowing on infection. Bull. Schizuoka Pref. Citrus Exp. Stn. 11:54-67.
19. Serizawa, S., Inoue, K., and Goto, M. 1969. Studies on citrus canker I. Dispersal of the citrus canker organism. Bull. Schizuoka Pref. Citrus Exp. Stn. 8:81-85.
20. Vanderplank, J. E. 1963. Plant Diseases: Epidemic and Control. Academic Press, New York. 349 pp.